Climate Dynamics (2002) 18: 501–517
DOI 10.1007/s00382-001-0190-z

C. Schnadt · M. Dameris · M.Ponater
R. Hein · V. Grewe · B. Steil

Interaction of atmospheric chemistry and climate and its impact on stratospheric ozone

Received: 8 March 2001 / Accepted: 21 June 2001 / Published online: 7 December 2001

Abstract The interactively coupled chemistry-climate model ECHAM4.L39(DLR)/CHEM is employed in sensitivity calculations to investigate feedback mechanisms of dynamic, chemical, and radiative processes. Two multi-year model simulations are carried out, which represent recent atmospheric conditions. It is shown that the model is able to reproduce observed features and trends with respect to dynamics and chemistry of the troposphere and lower stratosphere. In polar regions it is demonstrated that an increased persistence of the winter vortices is mainly due to enhanced greenhouse gas mixing ratios and to reduced ozone concentration in the lower stratosphere. An additional sensitivity simulation is investigated, concerning a possible future development of the chemical composition of the atmosphere and climate. The model results in the Southern Hemisphere indicate that the adopted further increase of greenhouse gas mixing ratios leads to an intensified radiative cooling in the lower stratosphere. Therefore, Antarctic ozone depletion slightly increases due to a larger PSC activity, although stratospheric chlorine is reduced. Interestingly, the behavior in the Northern Hemisphere is different. During winter, an enhanced activity of planetary waves yields a more disturbed stratospheric vortex. This "dynamical heating" compensates the additional radiative cooling due to enhanced greenhouse gas concentrations in the polar region. In connection with reduced stratospheric chlorine loading, the ozone layer clearly recovers.

C. Schnadt · M. Dameris (✉) · M. Ponater
R. Hein · V. Grewe
DLR Institut für Physik der Atmosphäre,
Oberpfaffenhofen,
82230 Weßling, Germany
E-mail: martin.dameris@dlr.de

B. Steil
Max-Planck-Institut für Chemie,
Abteilung Luftchemie,
55020 Mainz, Germany

1 Introduction

Extensive investigations have been made of how changes of the concentrations of radiatively and chemically active gases affect the radiative, chemical, and dynamic behavior of the stratosphere and their feedback on climate (e.g. Ramanathan et al. 1976; Groves et al. 1978; Boughner 1978; Fels et al. 1980; Shine 1986, 1989). Of particular interest has been the mutual effect of ozone and climate change (e.g. Cariolle et al. 1990; Dameris et al. 1991; Pitari et al. 1992; Graf et al. 1998). Increased attention has been focused recently on the substantial reduction of the ozone layer during the past two decades and its relevance for climate change (e.g. Bengtsson et al. 1999; Forster 1999; Randel and Wu 1999; Langematz 2000). Currently, the timing and the completeness of ozone recovery over the coming years and decades is very uncertain. On one hand, the recovery of the ozone layer will depend on the chlorine loading of the stratosphere, which is expected to decrease during the next decades (WMO 1999). On the other hand, climate change, which is expected as a consequence of the anticipated further increase of greenhouse gas concentrations, may become relevant for atmospheric ozone chemistry in the future (e.g. Shindell et al. 1998; Danilin et al. 1998; Dameris et al. 1998; Austin et al. 2000). Austin et al. (1992) were the first to discuss the possibility of an Arctic ozone hole in a doubled CO_2 atmosphere as a consequence of a reduced lower stratospheric temperature. Their model study clearly indicated that a strong radiative perturbation in the stratosphere has a distinct effect on ozone destruction. Therefore, investigating the interaction of climate change and of ozone recovery is one of the major scientific challenges of present day climate research.

In fact, long-term temperature measurements show a statistically significant warming of lower tropospheric layers and a pronounced cooling of the stratosphere. Both trends can be partly explained by the observed

increase of greenhouse gas concentrations during the last century (e.g. Steinbrecht et al. 1998; Pawson et al. 1998; Kivi et al. 1999; Santer et al. 1999). The cooling of the Arctic and Antarctic stratosphere is clearly enhanced due to ozone depletion itself, particularly in late winter and spring, which is obvious from multi-year data records (e.g. Randel and Wu 1999; WMO 1999). These temperature changes are associated with an increased stability of the wintertime stratospheric polar vortices and a poleward shift of the westerly wind belts near the surface (Hartmann et al. 2000). As other recent findings point out, the modelling of the atmospheric system must not only consider the feedback mechanisms of dynamic, chemical, and radiation processes in the stratosphere as a secluded system, but it must also take into account the dynamic coupling between the troposphere and the stratosphere. This dynamic link and its importance for the genesis of natural and anthropogenic climate variations have been intensively analyzed in a series of investigations (e.g. Perlwitz and Graf 1995; Perlwitz et al. 2000). For example, it was shown that winter seasons characterized by either a strong or a weak stratospheric vortex are associated with different tropospheric circulation regimes. On the other hand, upward propagating planetary waves originating in the troposphere have a dominant influence on the dynamic behavior of the stratosphere due to wave breaking and momentum deposition (e.g. Andrews et al. 1987).

In this study the interactively coupled chemistry-climate model ECHAM4.L39(DLR)/CHEM (hereafter referred to as E39/C) is used to obtain further knowledge about dynamic and chemical key processes involved in the recent changes of tropospheric and lower stratospheric temperature and chemical composition, and to provide indications for the possible development of climate and its impact on the ozone layer in the near future. Considering the feedback between dynamic, chemical, and radiative processes establishes a clear conceptional progress for climate change studies compared with conventional general circulation models (GCMs), which use fixed climatological mean fields of short-lived radiatively active chemical species like ozone (e.g. Bengtsson et al. 1999) in the model's radiative transfer scheme. Furthermore, the application of a chemistry model that considers relevant chemical species and reactions to describe upper troposphere and lower stratosphere ozone chemistry (instead of much simpler approaches with parameterized chemistry, e.g. Cariolle et al. 1990; Shindell et al. 1998) in multi-year simulations is another step forward to obtain a better understanding of the reasons for observed changes of climate parameters and the chemical composition of the atmosphere.

Our aim is to identify and to investigate important interaction mechanisms between dynamic, chemical, and radiative processes in the lower stratosphere. Due to their importance for polar stratospheric ozone, feedback mechanisms in the polar stratosphere during winter and spring are of particular interest. Thus their investigation constitutes the essential part of this paper. The analysis is based on scenario calculations, which include the changes of atmospheric composition during recent years, mainly resulting from greenhouse gas concentration increases and changes of stratospheric chlorine loading. By comparing these numerical experiments, changes of dominant interaction mechanisms and their impact on stratospheric ozone can be identified. At first, an adequate comparison between model results of multi-year integrations and respective long-term observations forms the basis for the analysis of dynamic-chemical interaction mechanisms.This indicates the comprehensiveness of our understanding of the atmospheric system, and it also shows the abilities and deficiencies of the model system employed.

Such a comparison of model results to related observations has shown that the model is able to describe important dynamic and chemical processes and to reproduce the seasonal and spatial distribution of relevant chemical species (Sect. 3.1) for recent atmospheric conditions (Hein et al. 2001, hereafter referred to as H2001). This scenario run will be designated 'reference simulation'. Here, E39/C is used to investigate changes of dynamics and chemistry in the past and future compared with this reference simulation. The work is subdivided into two parts: first, an extended model valuation is presented, which shows the model's performance in reproducing observed stratospheric temperature, ozone, and water vapor trends of the 1980s. The second part deals with dynamic and chemical changes that arise as a consequence of enhanced greenhouse gas concentrations and a slightly reduced stratospheric chlorine abundance (with respect to the reference simulation) in a near future scenario.

In the following section a brief summary of the model and the design of the experiments will be presented. Model results will be discussed and compared with observations in Sect. 3. The radiative and dynamic processes, which are responsible for the behavior of the model will be investigated in the subsequent section. Conclusions will be given in the last section.

2 Brief model description and design of experiments

2.1 The model

A detailed description of the chemistry-climate model E39/C, the used parameterisations, boundary conditions, as well as natural and anthropogenic emissions was given in H2001. They also discussed the main features of the model climatology. In this section the model characteristics are briefly summarized.

The atmosphere GCM ECHAM4.L39(DLR) (E39) is applied with a horizontal resolution of T30, i.e. dynamic processes have an isotropic resolution of about 670 km. The corresponding Gaussian transform latitude-longitude grid, on which the model physics, chemistry, and tracer transport are calculated, has a mesh size of 3.75°×3.75°. In the vertical, the model uses 39 layers (L39) from the surface up to the top layer centred at 10 hPa (Land et al. 1999). No adjustment of the temperatures, which would improve

the agreement with observations has been employed in E39/C to keep self-consistent results within the fully interactively coupled model system. The applied chemistry model CHEM (Steil et al. 1998) is based on the family concept. It contains the most relevant chemical compounds and reactions necessary to simulate upper tropospheric and lower stratospheric ozone chemistry, including heterogeneous chemical reactions on polar stratospheric clouds (PSCs) and sulfate aerosol, as well as tropospheric NO_x-HO_x-CO-CH_4-O_3 chemistry. CHEM has been employed in an updated version, as described in H2001. It does not consider bromine chemistry. Physical, chemical, and transport processes are calculated simultaneously at each time step, which is fixed at 30 min. This is a favourable compromise with respect to similar model systems, which employ simplified chemistry parameterizations to enable multi-year simulations. Since E39/C allows us to study chemistry-climate feedback mechanisms in decadal integrations it has an advantage over model systems which must be restricted to shorter simulations of specific episodes due to a necessary shorter timestep in chemistry.

Nitrogen oxide ($NO_x = NO + NO_2$) emissions at the Earth's surface (both natural and anthropogenic), from lightning, and from aircraft are considered. Methane (CH_4), nitrous oxide (N_2O), and carbon monoxide (CO) mixing ratios are prescribed at the surface. Monthly mean concentrations of chlorofluorocarbons (CFCs) depending on latitude and altitude, and upper boundary values for total chlorine ($ClX = HCl + ClONO_2 + ClO_x$, $ClO_x = Cl + ClO + ClOH + 2{\cdot}Cl_2O_2 + 2{\cdot}Cl_2$) and total nitrogen ($NO_y = NO_x + N + NO_3 + 2{\cdot}N_2O_5 + HNO_4 + HNO_3$) are taken from results of the Mainz two-dimensional model of Brühl and Crutzen (1993). The upper boundary conditions account for transport and chemical reactions above the model domain. They are largely responsible for the lower stratospheric nitrogen oxides and chlorine concentrations. E39/C includes an online feedback of chemistry, dynamics, and radiative processes: chemical tracers are transported by the simulated winds and the net heating rates are calculated using the actual concentrations of the radiatively active gases O_3, CH_4, N_2O, CFCs, and water vapor (H_2O).

Sea surface temperature (SST) distributions are prescribed for the various time slices according to the transient climate change simulations of Roeckner et al. (1999, see Sect. 2.2). The impact of stratospheric ozone changes and water vapor changes from methane oxidation on the troposphere-surface system was not accounted for in Roeckner et al.'s (1999) simulations and is, hence, not included in the SST changes prescribed for our scenarios.

2.2 Design of experiments

For the current investigations, E39/C simulations for three time slices are analyzed. Each model experiment is run in steady state, representing conditions for 1980, 1990, and 2015, respectively. After a spin-up period of four years, each simulation is integrated over 20 annual cycles. The model data of these 20 years (model years 5 to 24) are evaluated. They are compared with observations and with each other to study the changes of the atmosphere caused by modified concentrations of chemically active compounds. The "1990" scenario, which is used as the reference simulation, has already been analyzed in detail by H2001. Here, a valuation with observations is carried out for the differences between the "1990" and the "1980" experiments, focusing on the ability of the coupled model system to reproduce the temporal development of dynamic and chemical values, especially at polar latitudes of both hemispheres. The "2015" simulation is applied to study the response of the evaluated model system to expected future changes of stratospheric chlorine loading and greenhouse gas concentrations.

Table 1 Mixing ratios of greenhouse gases and NO_x emissions of different natural and anthropogenic sources adopted for the model simulations

	1980	1990	2015
CO_2 [ppmv]	337	353	405
CH_4 [ppmv]	1.57	1.69	2.05
N_2O [ppbv]	303	310	333
Cl_y [ppbv]	2.3	3.4	3.1
NO_x lightning (Tg(N)/year)	5.2	5.3	5.6
NO_x air traffic (Tg(N)/year)	0.3	0.6	1.1
NO_x surface (total) (Tg(N)/year)	29.9	33.1	43.8
NO_x surface (industry, traffic)	19.5	22.6	32.9
NO_x surface (soils)	5.5	5.5	5.5
NO_x surface (biomass burning)	4.9	5.0	5.4

Table 1 gives an overview of the individual boundary conditions for the three scenario simulations. The design of the model simulation "1990" and the references for the respective boundary conditions, as well as the emissions have been described by H2001. They are taken from recognized publications, which are mainly based on observations. The boundary values of the most relevant greenhouse gases (CO_2, N_2O, CH_4) for "1980" and "1990" are taken from IPCC (1990). Respective values for the "2015" scenario are prescribed according to the IPCC-scenario IS92a (business-as-usual, IPCC 1996). The upper boundary values for NO_y and ClX, as well as the zonal CFC fields stem from a transient simulation of the Mainz 2D model (cf. above) for all three scenarios. They are adapted to observations for "1980" and "1990" and follow projected changes for "2015" (WMO 1999). The development of the CFC concentrations is prescribed on the basis of recent measurements of tropospheric CFC concentrations (e.g. Montzka et al. 1996, 1999), indicating that a decrease from 1990 to 2015 of approximately 10% can be expected. This assumption is reflected by the calculated average stratospheric total inorganic chlorine (Cl_y), which shows a decrease from 3.4 ppbv in "1990" to 3.1 ppbv in "2015". The NO_x emissions from lightning are calculated online in the model, depending on cloud top height, as introduced by Price and Rind (1992, 1994). The emissions for the "1990" simulation have been scaled to provide a global mean value of nearly 5 Tg(N)/year, a value, which is in agreement with recent estimates (e.g. Huntrieser et al. 1998). Moderate changes of NO_x emissions from lightning in the two other simulations are caused by an altered climate, which modifies the simulated frequency and strength of convective events and, therefore, the respective NO_x production. The annual surface emissions from biomass burning, industry, and traffic for the "1980" and "2015" time slices are constructed on the basis of the data used for the "1990" simulation (Benkovitz et al. 1996), considering real past and expected future global growth rates (IPCC 1999). The global NO_x soil emissions by micro-biological production are identical in the three simulations. NO_x emissions from air traffic are considered, employing the data sets provided by Schmitt and Brunner (1997) for the years 1990 and 2015. For the "1980" simulation an increase of approximately 7%/year of the world wide civil air traffic during the 1980s has been assumed (A. Schmitt personal communication) yielding roughly a 100% increase from 1980 to 1990. The atmospheric aerosol loading is considered to be equal in the three scenarios.

Climatological mean values of the sea surface temperatures (SSTs) have been calculated from observations for the years 1979–1994 (AMIP period: Gates 1992). They are prescribed in the "1990" model simulation. The SSTs for the "1980" and the "2015" simulations have been constructed on the basis of a transient climate run with the coupled atmosphere-ocean GCM ECHAM4/OPYC (Roeckner et al. 1999). Their experiment was also run with greenhouse gas increases according to IS92a, hence the SST trends prescribed in our scenarios are consistent with the prescribed greenhouse gas concentrations. Temporal mean SSTs from the transient ECHAM4/OPYC run have been calculated for two 10-year periods (1976 to 1985, 2011 to 2020). SST differences referring to these periods are added to the SST reference distribution used in our "1990" simulation, yielding the employed SST fields adopted in the "1980" and the "2015" scenarios.

3 Description of model results

3.1 Main features of the reference experiment "1990"

The valuation of the "1990" reference simulation (H2001) has generally yielded a satisfactory description of dynamic and chemical processes and parameter distributions. In particular, in the Northern Hemisphere the modelled lower stratospheric dynamics have shown good agreement with observations, i.e. the high dynamic interannual variability including the occurrence of stratospheric warmings has been reproduced, as well as the subsidence of air masses inside the winter vortex. The increased number of atmospheric model layers compared with earlier model versions, particularly near the tropopause and in the lower stratosphere, obviously results in improved transport characteristics (Timmreck et al. 1999; Land et al., submitted). The simulated distributions of relevant chemical compounds (particularly ozone) have been found to be conformable with satellite and radiosonde measurements. This is a considerable improvement compared with the previously used model version (Steil et al. 1998; Grewe et al. 1998) which had a reduced spatial resolution and which neglected the feedback of dynamic and chemical processes. Considering the interaction of chemistry and climate at each time step has yielded a substantial progress regarding the distribution of stratospheric water vapor, which is important for a realistic description of polar chemistry.

H2001 have also reported some model deficiencies, many of which appear to be closely related to a cold bias in the polar stratosphere in Southern Hemisphere winter and spring. For example, the too cold and too stable Southern Hemisphere polar vortex in the stratosphere is associated with a delayed vortex breakdown (final warming) and, therefore, the ozone depletion over Antarctica extends too far into spring. This "cold-bias" problem has often been considered as being typical for GCMs with model top at 10 hPa. Sometimes, the use of such models for coupled chemistry-climate simulations has even been questioned in general (Austin et al. 1997; Rind et al. 1998) due to their inability to give full account of the stratospheric mean meridional circulation (overturning). This verdict does not do justice to the favourable E39/C results which are gained especially for the Northern Hemisphere as presented in H2001, which they mainly relate to enhanced vertical resolution (see also Rind et al. 1998). It should also be recalled that the cold bias is present in a number of middle atmosphere GCMs, too (e.g. Austin et al. 2000; Pawson et al. 2000). We will return to the importance of vertical resolution and location of the model top in the concluding discussion.

While the "1990" reference simulation with E39/C fairly reproduces many dynamic features that are considered fundamental for a reasonable description of the distribution of active and passive tracers, this does not assure an equally fair reproduction of observed trends. Thus, a specific trend valuation will be presented in the next subsection.

3.2 Changes in the past: comparison with observations

In this section the reference experiment "1990" (H2001) and the "1980" scenario run are used to analyze the model's ability to reproduce the temporal development of dynamic and chemical parameters and processes during the most recent past. Emphasis is given to phenomena and processes relevant for stratospheric ozone chemistry. Figure 1 shows the differences of the zonal and annual mean temperature between the two simulations. Negative values indicate a cooling of the atmosphere from "1980" to "1990". Obviously, the results demonstrate the well-known typical pattern with a warming of the troposphere and a cooling of the stratosphere due to the greenhouse effect (e.g. Rind et al. 1990; Mahfouf et al. 1994; Roeckner et al. 1999; Grewe et al. 2001). Temperature changes in polar regions are particularly important for stratospheric ozone depletion and are, hence, shown in more detail in Fig. 2, including the vertical and annual structure. A univariate statistical test (*t*-test) suggests that the tropospheric warming at high latitudes is not significant for most of the time, either in the Northern Hemisphere (Fig. 2a) or in the Southern Hemisphere (Fig. 2b), except for the summer months at northern latitudes. Nevertheless, the strength of the middle tropospheric temperature changes is in agreement with observations (e.g. Steinbrecht et al. 1998; WMO 1999). During southern spring a marked cooling of the Antarctic lower stratosphere is simulated by the model (Fig. 2b). Peak values of –9 K are found at 40 hPa in November. This finding is in agreement with an analysis of Randel and Wu (1999, see their Fig. 11a) whose investigations of the NCEP re-analysis data (1993–97 minus 1970–79) have shown a similarly strong cooling (–8 K) during the same month. The Southern Hemisphere cooling pattern in model data and observations also looks very similar: The cooling starts at higher altitudes in spring after sunrise, and it penetrates down to lower atmospheric layers in the following three months. However, the NCEP data show the strongest cooling around 100 hPa, which is clearly below the region of maximum cooling in the model. The significantly enhanced cooling is linked to the strong ozone depletion in this region (not shown). Randel and Wu's (1999) analysis shows similarly strong temperature decreases in the Northern Hemisphere spring (their Fig. 11b), which are not reproduced by the model (Fig. 2a). Corresponding temperature differences calculated from E39/C data ("1990" minus "1980") do not indicate a statistically significant change during winter and spring. It must be emphasized that the high dynamic interannual vari-

ability of the Northern Hemisphere makes it very difficult to obtain reliable trend estimates. This was demonstrated by Labitzke and v. Loon (1994, 1995). In a detailed analysis of temperature variations in the Northern Hemisphere lower stratosphere (100–10 hPa) between 1964 and 1993 they showed that the linear temperature trends are neither uniform in latitude nor in season, and that large fluctuations on a decadal scale are obvious. In the Northern Hemisphere, a calculated trend crucially depends on the beginning and ending of the time series analyzed (Labitzke 2000 personal communication). In this context it must be kept in mind that the analysis of the NCEP data contain the extraordinary cold northern winters in the 1990s, which dominate the strength and shape of the temperature differences between the adopted time intervals. The reasons for these unusually cold winters are still not known.

Figure 3 illustrates how the corresponding time development of temperature, ozone, and activated chlorine (ClO_x) in the polar vortices is captured by the model. Based on 20-year means of daily values it shows differences of the two simulations "1980" and "1990" at 50 hPa in the Southern Hemisphere (July to November) and in the Northern Hemisphere (December to April). For an appropriate presentation of the results, especially in the Northern Hemisphere, the zonal mean values of the standard coordinate system are transformed to a description employing equivalent potential vorticity (PV) coordinates (e.g. Butchart and Remsberg 1986; Manney et al. 1994a). Temperature differences (Fig. 3a, b) indicate a significant cooling in Antarctic spring (compare to Fig. 2), but no clear changes are obvious inside the Northern Hemisphere polar vortex until April, where a marginally significant temperature decrease of –3 to –4 K might indicate a more persistent vortex in "1990" than in "1980". The temperature decrease in Southern Hemisphere spring is evidently accompanied by a pronounced ozone reduction (up to –1.4 ppmv, Fig. 3c), which amounts to an approximate 70% relative change at 50 hPa. In the Northern Hemisphere polar region ozone depletion is enlarged by about –16% between late March and early April (Fig. 3d). It is interesting to note that the model also reproduces some additional ozone reduction outside the polar vortex (30°N-60°N equivalent latitude) in February and March, which is statistically significant (95%-significance level). This is probably due to a combination of an increased catalytic ozone destruction by ClO_x and HO_x radicals, as well as a transport of ozone depleted air masses out of the vortex (vortex erosion) (Grewe et al. 1998).

In both hemispheres chlorine activation is significantly enhanced inside the vortices (Fig. 3e, f), which is proportional to the prescribed 45% increase of Cl_y (see Table 1). The ClO_x change pattern evolves differently in both hemispheres: in the Southern Hemisphere the highest mixing ratios are found at the inner edge of the polar vortex. This is the region where the conditions are most

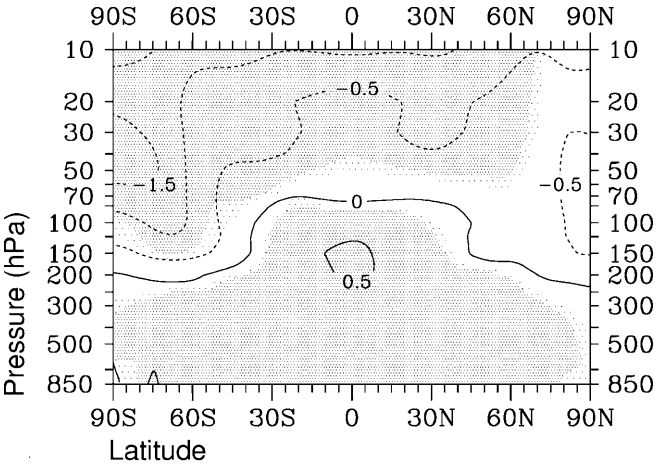

Fig. 1 Difference of climatological annual mean temperatures (in K) determined from the "1990" and "1980" simulations. *Light (dark) shading* indicates regions in which differences are statistically significant at the 95% (99%) level

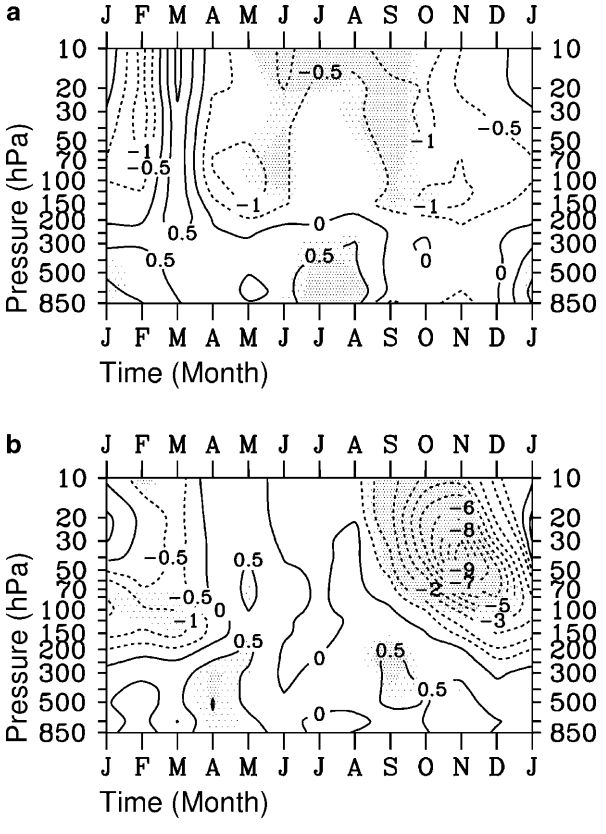

Fig. 2a,b Temperature differences (in K) ("1990" minus"1980") **a** at 80°N and **b** at 80°S depending on altitude and season. *Heavy (light) shaded areas* indicate the 99% (95%) significance level (*t*-test)

favourable for the formation of PSCs. PSC formation in the model is strongly dependent on temperature, and mixing ratios of nitric acid and water vapor (Steil et al. 1998). In mid-winter, the centre of the Southern Hemi-

sphere vortex is almost completely denoxified and strongly dehydrated, associated with the low temperatures in this region. Under these circumstances, the formation of PSCs and thus chlorine activation is restricted. Inside the Northern Hemisphere polar vortex throughout the winter and spring period, highest ClO_x mixing ratios are simulated nearer to the core region of the vortex. Here, both dehydration and denoxification are not as large as in the Southern Hemisphere.

The change of ozone columns between the "1980" and "1990" simulations is presented in Fig. 4. As expected, the most pronounced decrease of total ozone is computed during southern polar springtime with values up to –26%. At high latitudes of the Northern Hemisphere, total ozone is reduced by approximately –4% between mid January and April. Due to the high interannual dynamic variability of the Northern Hemisphere polar stratosphere, however, the changes are not statistically significant at most locations throughout the time of the year mentioned. Smallest changes are found at tropical latitudes where total ozone reductions amount to less than –2%. The modelled ozone trend is in good agreement with an analysis of the 16-year (1978–1994) combined Nimbus 7/Meteor 3 TOMS version 7 ozone record (McPeters et al. 1996). The model results for the Southern Hemisphere, for the tropical region, and for the subtropics of the Northern Hemisphere show a correct reproduction of the percentage decrease of total ozone. In extra-tropical northern latitudes the decrease of ozone columns is somewhat underestimated by the model. Considering the high interannual dynamic variability of this region however, the model results are in satisfying agreement with the observed ozone trend.

To investigate the height dependence of modelled ozone changes between "1990" and "1980" in more detail, differences of zonal mean ozone mixing ratios are presented in Fig. 5, showing ozone changes for March (Fig. 5a) and for October (Fig. 5b). In the troposphere, mixing ratios are obviously higher in "1990" than in "1980" (5–10 ppbv) due to the adopted higher NO_x emissions, particularly at middle and high latitudes of the Northern Hemisphere. The modelled tropospheric ozone increase is consistent with the measured ozone trend at most mid-latitude radiosonde stations (WMO

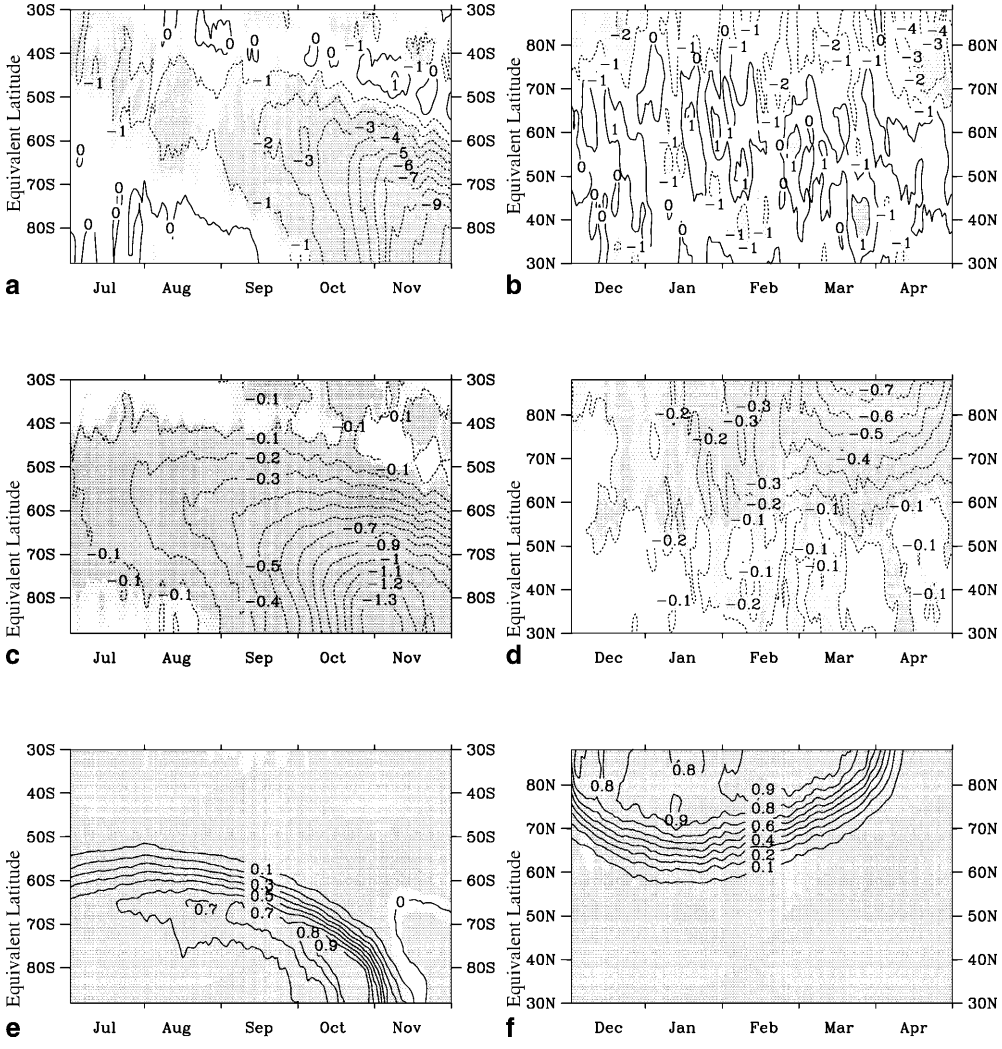

Fig. 3a–f Changes of temperature (*top*, in K), ozone (*middle*, in ppmv), and activated chlorine (*bottom*, in ppbv) at 50 hPa in the Southern (*left*; July to November) and in the Northern Hemisphere (*right*; December to April), as calculated from the model simulations "1990" and "1980". *Negative (positive) values* indicate higher (lower) values in "1980" ("1990"). Model data are transformed to PV-coordinate system (see text). *Heavy (light) shaded areas* indicate the 99% (95%) significance level (*t*-test)

1998). E39/C does not reproduce the different behavior between Canadian and European stations, as indicated by the analysis of the period between the years 1970 and 1996, where the Canadian radiosonde stations found a slight decrease of tropospheric ozone concentrations. In the lower stratosphere, ozone mixing ratios in the model are clearly reduced, indicating the strongest ozone depletion at polar latitudes of both hemispheres. The strongest ozone reduction is simulated at a slightly higher altitude than observed (WMO 1999), particularly in Antarctic spring. This may be caused by an underestimated subsidence and related temperature cold bias of the model in this region.

At the end of this subsection we present climatological zonal means of water vapor mixing ratios of the "1990" scenario (Fig. 6a, b) and respective trends between the simulations "1990" and "1980" (Fig. 6c, d) for solstice conditions. The results of the reference simulation "1990" indicate that E39/C is able to qualitatively reproduce the observed lower stratospheric water vapor distribution, which is characterized by a positive meridional gradient, i.e. higher mixing ratios in the extra-tropics than in tropical regions. Compared with HALOE measurements, however, it is much weaker in our model (H2001). The modelled dehydration of the Antarctic winter lower stratosphere is overestimated (Fig. 6b, by approximately 1 ppmv, see also discussion in H2001) as a consequence of the mentioned cold bias in this region. An important question is how the water vapor mixing ratio develops in the model, particularly in polar regions. For example, Chipperfield and Pyle (1998) showed that a modelled Arctic ozone depletion could increase due to an enhanced PSC activity when the stratospheric H_2O loading is enhanced. Figure 6c, d shows that tropospheric and lower stratospheric water vapor mixing ratios increase from "1980" to "1990". The overall rise of H_2O is mainly caused by the prescribed methane increase and the resulting enhanced chemical water vapor production by methane oxidation.

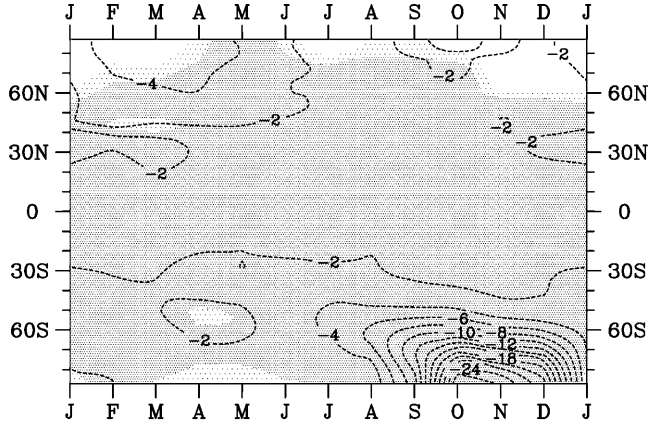

Fig. 4 Relative difference (in %) of climatological zonal mean total ozone ("1990" minus "1980") depending on latitude and season. *Shaded areas* mark the regions of statistically significant changes

In polar latitudes of the winter stratosphere the changes of water vapor mixing ratios are not significant in E39/C. Indeed, the area covered by PSCs is clearly larger in "1990" (not shown), which indicates a stronger PSC activity than in "1980". On the other hand, the larger amount of PSCs yields a more effective dehydration, which compensates part of the chemical water vapor production.

The only available multi-year data record of upper troposphere/lower stratosphere water vapor, which can be used for reliable trend analysis and for comparison with model changes was reported by Oltmans and Hofmann (1995). They showed a significant increase of water vapor mixing ratios in the lower stratosphere above Boulder (40°N, 105°W) between 1981 to 1994, which refers to 0.8%/year at 19 km (0.3 ppmv/decade). This is the same order of magnitude as simulated by E39/C, indicating that the model results reproduce the trend analyzed by Oltmans and Hofmann (1995).

3.3 Near future changes

Having shown that the interactively coupled chemistry-climate model E39/C reasonably reproduces prominent

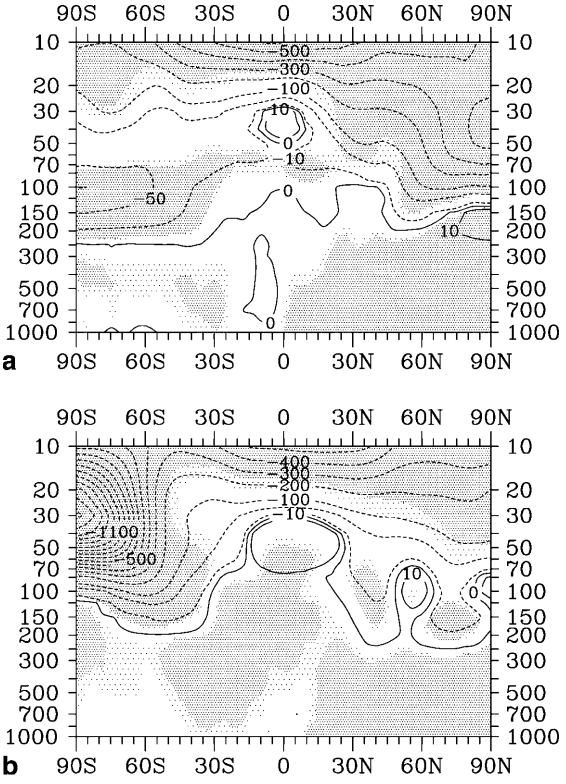

Fig. 5a,b Changes of the climatological zonal mean ozone mixing ratios (in ppbv) for the "1990" and the "1980" simulation depending on altitude and latitude for **a** March and **b** October. *Negative (positive) values* indicate higher (lower) values in "1980" ("1990"). *Heavy (light) shaded areas* indicate the 99% (95%) significance level (*t*-test)

features of observed dynamic and chemical trends during the recent past, a sound basis is formed to simulate the development of key parameters and processes for possible future conditions. As the impact of climate change on the recovery of the stratospheric ozone layer is not yet completely understood and subject to debate, model simulations like ours will help to assess the relative importance of various processes. At least four mechanisms are incorporated in our model: temporal development of atmospheric chlorine loading, of stratospheric water vapor, of stratospheric temperature and circulation due to CO_2, CH_4, N_2O, O_3, and water vapor changes, and of increasing NO_x mixing ratios due to surface, aircraft, and lightning emissions (see Table 1).

Figure 7 displays the temperature changes determined by the differences of the zonal mean climatological temperatures of the "2015" and "1990" simulations. The general pattern found equals the result presented in Fig. 1 ("1990" minus "1980") indicating a warming of the troposphere and a cooling of the lower stratosphere. Temperature differences between "1990" and "2015" are larger than the respective changes between "1980" and "1990", which is consistent with the prescribed increase of greenhouse gas concentrations in the different model simulations (Table 1). It should be noticed that the annual mean temperature changes in the Northern Hemisphere polar stratosphere are not statistically significant, which is explained by the strong dynamic variability of this region, particularly in winter. Figure 8 shows temperature changes between "1990" and "2015" in the polar regions (see also Fig. 2). Two remarkable features are visible: (a) a warming of the lower stratosphere (more than +4 K) is found in the Northern Hemisphere during winter, which is statistically significant (95% significance level) in February below 30 hPa; (b) the Southern Hemisphere stratospheric temperature change pattern is similar to that shown in Fig. 2b, except that the maximum temperature decrease (–7 K) is found in December (instead of November) and at a lower altitude (50 hPa instead of 40 hPa). This result gives a first indication that the southern polar vortex in "2015" is more persistent than it is in "1990" (see later).

The ozone column changes of the climatological mean fields in the "1990" and the "2015" simulations are presented in Fig. 9. Whereas the Northern Hemisphere generally shows a significant increase of total ozone, a slight further decrease of ozone columns is found in the Southern Hemisphere lower and middle latitudes, which is statistically significant at least for some months and latitudes. Maximum changes are visible at high latitudes of both hemispheres. In "2015", the ozone column over the south polar region shows a further reduction of about –10% (most pronounced in October by up to –14%), whereas total ozone is markedly increased by about 8% at Northern Hemisphere polar latitudes. Obviously these ozone changes are connected to the simulated temperature changes shown in Fig. 8. We will now analyze and discuss various interacting effects to explain the interhemispheric differences in total ozone development.

Southern hemispheric differences of 20-year averaged daily values between the two simulations are displayed in Fig. 10 for temperature, O_3, ClO_x, HCl, $ClONO_2$, and HNO_3 at 50 hPa from July to Novem-

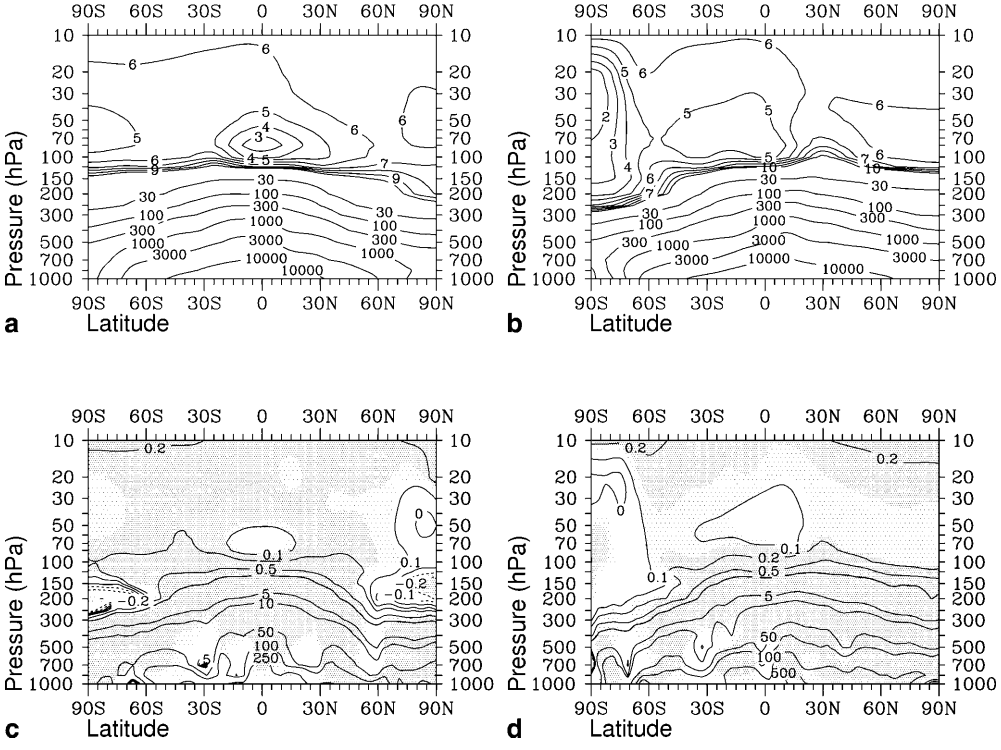

Fig. 6a–d Climatological mean water vapor mixing ratios (in ppmv) for the reference simulation "1990", for **a** Northern Hemisphere winter (DJF) and for **b** summer (JJA) conditions. Differences with respect to the "1980" simulation are displayed in **c** for DJF and in **d** for JJA. *Positive values* indicate an increase of mixing ratios from "1980" to "1990"

ber. As already explained (Fig. 3), the model data have been transformed to PV-coordinates. Ozone mixing ratios (Fig. 10b) continue to decrease by up to –0.6 ppmv from "1990" to "2015", resulting in mean polar ozone mixing ratios of less than 0.5 ppmv in the "2015" simulation at the centre of the polar vortex in October (not shown). ClO_x (Fig. 10c) is significantly increased at the inner edge of the vortex in "2015". The observed general picture of low HNO_3 mixing ratios inside the vortex surrounded by a "collar" of high HNO_3 values (e.g. Toon et al. 1989; Santee et al. 1999), which is reproduced by the model (not shown), is markedly enhanced (Fig. 10f) in "2015": the increased HNO_3 mixing ratios outside the vortex (collar region) are caused by the generally amplified NO_x emissions in "2015", and by increased NO_y values at the model upper boundary, representing nitrogen oxides produced by the N_2O photodissociation above the model top. At the inner edge of the polar vortex an additional decrease of gaseous HNO_3 (denoxification) is found due to an intensified formation of PSCs, which reflects the enhanced radiative cooling of the lower stratosphere in the "2015" scenario. Evidently, the enhanced ozone loss from the temperature driven PSC increase (see Fig. 10a) outweighs the ozone recovery that would arise from the chlorine decrease alone. Cooling at southern higher latitudes is particularly intensified after mid October due to radiative feedback from the enlarged and more persistent ozone hole (Fig. 10a). An interesting feature can be noticed with respect to the subsequent recovery of the chlorine reservoirs HCl and $ClONO_2$ (Fig. 10d, e): at the end of October when ozone mixing ratios in polar latitudes fall below 0.5 ppmv, negative (positive) changes of $ClONO_2$ (HCl) are found. The model apparently reproduces a mechanism discussed in detail by Douglass et al. (1995): if the O_3 mixing ratio falls below about 0.5 ppmv in the strongly denitrified core region of the Southern Hemisphere polar vortex, HCl increases rapidly at the expense of $ClONO_2$. Under these circumstances, the formation of ClO and the subsequent recombination of

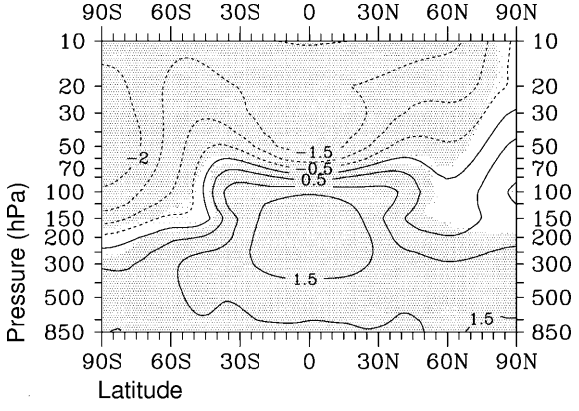

Fig. 7 Same as Fig. 1, but determined from the simulations "2015" and "1990"

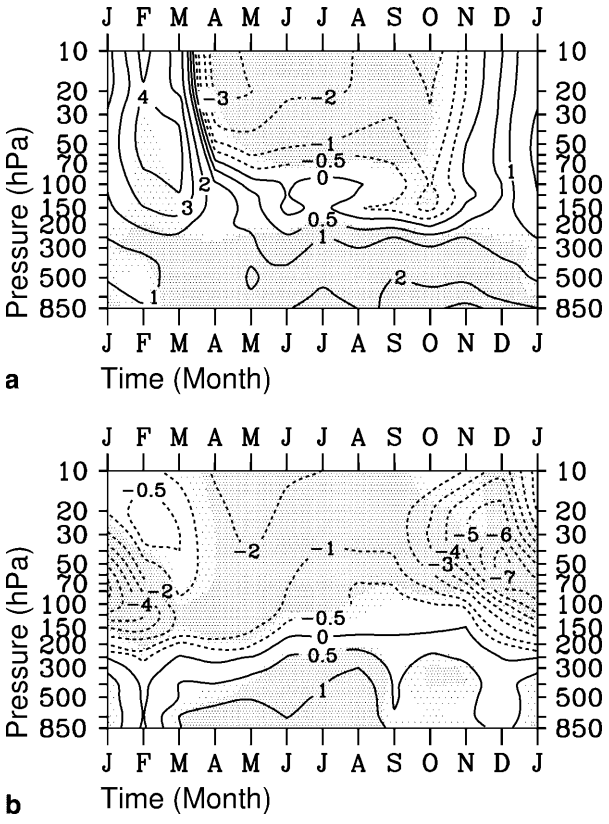

Fig. 8a,b Same as Fig. 2, but determined from the simulations "2015" and "1990"

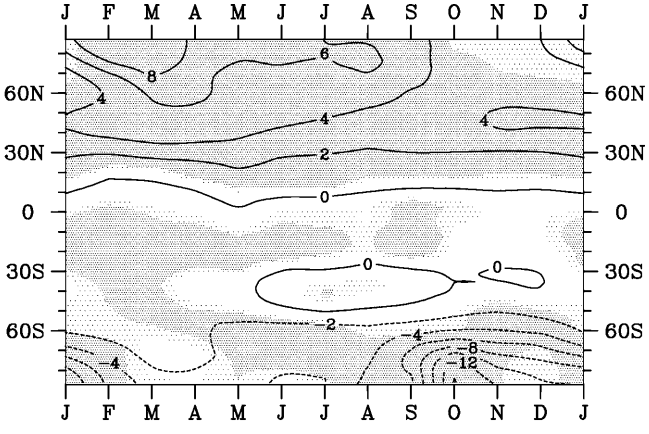

Fig. 9 Same as Fig. 4, but determined from the simulations "2015" and "1990"

$ClONO_2$ become negligible. The change of reservoir gas partitioning is accompanied by an earlier decrease of ClO_x.

A distinctly different picture is found in the Northern Hemisphere lower stratosphere (Fig. 11). No significant ozone changes can be found in the centre of the polar vortex before mid February (Fig. 11b), while a pronounced increase of ozone mixing ratios occurs in spring with maximum values of $+0.7$ ppmv in the vortex centre at the end of March. This is consistent with the decline

of ClO_x mixing ratio (Fig. 11c) inside the polar vortex during the winter months. In contrast to the conditions in the Southern Hemisphere winter, the 50 hPa temperatures do not significantly change until the end of February (Fig. 11a), although the greenhouse gas concentrations in "2015" are enhanced. In March, temperatures inside the vortex are even higher in "2015" than in "1990" (up to +6 K), which is statistically significant. The temperature increase is accompanied by a chlorine deactivation (maximum decline of –1 ppbv in "2015" compared with "1990"). The key question whether dynamic or chemical processes are mainly responsible for this behavior of the simulated temperature will be discussed in detail in the subsequent section. No statistically significant changes between the two simulations are found for HCl, $ClONO_2$, and HNO_3 (Fig. 11d–f) inside the polar vortex. At middle and lower latitudes, higher HNO_3 mixing ratios are simulated due to the enhanced NO_x emissions and NO_y upper boundary values in "2015" as explained in the preceding section, whereas the lower HCl and $ClONO_2$ mixing ratios in these regions simply reflect the reduction of Cl_y.

An impression of ozone mixing ratio changes at different altitudes is shown in Fig. 12 for the months March and October. The prescribed enhancement of anthropogenic NO_x emissions results in a significant increase of tropospheric ozone, especially in the Northern Hemisphere. As mentioned above, lower stratospheric ozone changes are different in both hemispheres. Figure 12a indicates that the substantial increase of total ozone in Northern Hemisphere late winter and spring presented in Fig. 9 is not only caused by the lower stratospheric ozone increase discussed, but also by the enhancement of tropospheric ozone.

To complete our analysis, differences ("2015" minus "1990") of climatological water vapor mixing ratios for solstice conditions are presented in Fig. 13. A statistically significant increase of water vapor is simulated for the entire model domain for all seasons, except during Southern Hemisphere winter in the polar lower stratosphere, where a significant decrease (up to –0.5 ppmv) is simulated. The general increase of stratospheric H_2O values could be expected due to the prescribed enhancement of methane mixing ratios. However, part

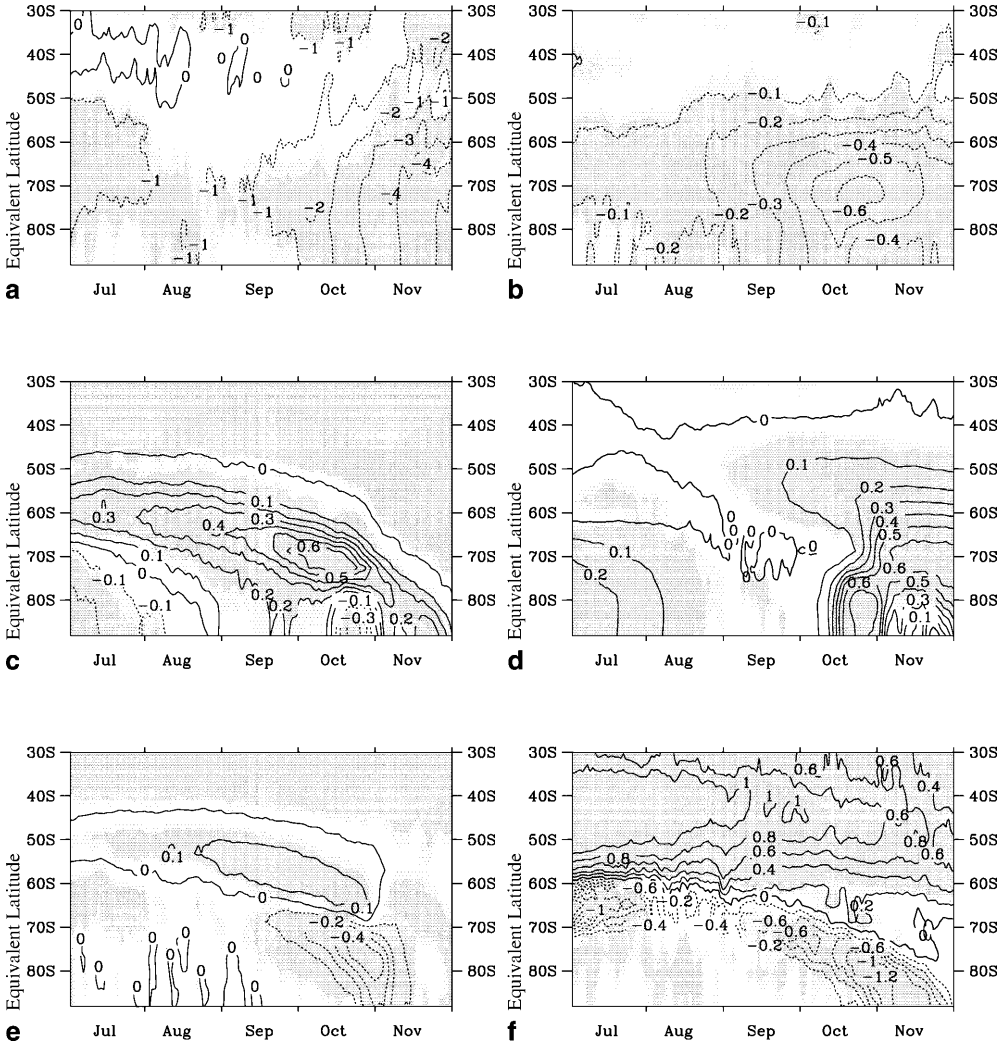

Fig. 10a–f Changes of **a** temperature (in K), **b** ozone (in ppmv), **c** ClO_x (in ppbv), **d** HCl (in ppbv), **e** $ClONO_2$ (in ppbv), and **f** HNO_3 (in ppbv) at 50 hPa in the Southern Hemisphere, as calculated from the model simulations "2015" and "1990" (July to November). *Negative (positive) values* indicate higher (lower) values in "1990" ("2015"). Model data are transformed to PV-coordinate system (see text). *Heavy (light) shaded areas* indicate the 99% (95%) significance level (*t*-test)

of the trend may also be caused by changes in stratospheric water vapor uptake from the troposphere due to increasing tropospheric temperature and water vapor or due to changing dynamic and thermodynamic conditions at the tropical tropopause. The enhanced dehydration in the Southern Hemisphere polar winter is consistent with the intensified local cooling (–1 to –2 K, Fig. 8b).

As mentioned in Sect. 2.1, the prescribed SST changes only represent the effect of homogeneous greenhouse gas increases throughout the period 1980 to 2015. They do not include the climate impact of stratospheric ozone changes and chemically induced stratospheric water vapor changes discussed. Hence, it may be worthwhile to consider the radiative forcing of these latter changes to give a first-order quantification of their relative importance for the total effect.

Table 2 shows the annual mean radiative forcing from all trace gas changes (as prescribed in or simulated by E39/C) as well as the individual contributions of stratospheric ozone and stratospheric water vapor. The values were calculated online in E39/C, using the method described by Stuber et al. (2001). According to the current conceptual theory (e.g. IPCC 1995) the radiative forcing has been determined at the topopause, after the stratospheric temperature has adjusted to a new equlibrium following the fixed dynamical heating assumption. The radiative forcing is given for the tracer changes in "1990" and "2015", relative to the "1980" concentrations.

4 Analyses of model results

We have demonstrated that our model system gives a consistent picture of the temporal development of the stratospheric ozone layer in accordance with the current knowledge about key processes and feedbacks. In view of the results of previous prognostic studies, one feature of our "2015" sensitivity experiment should be discussed in more detail: only in the Southern Hemisphere does the temperature response indicate the expected significant cooling of the lower stratosphere caused by the radiative feedback of enhanced greenhouse gas concentrations and its intensification by the strong ozone depletion in spring season (e.g. Zhou et al. 2000). Why does the model not indicate a cooling in the northern lower stratosphere for the "2015" simulation with respect to "1990", although the carbon dioxide and water vapor mixing ratios are enhanced? Does the simulation of a contrasting development of the ozone layer in the Northern and in the Southern Hemisphere represent a reliable estimate of future changes in the real atmosphere? In the following, additional analyses are presented and discussed with respect to radiative and

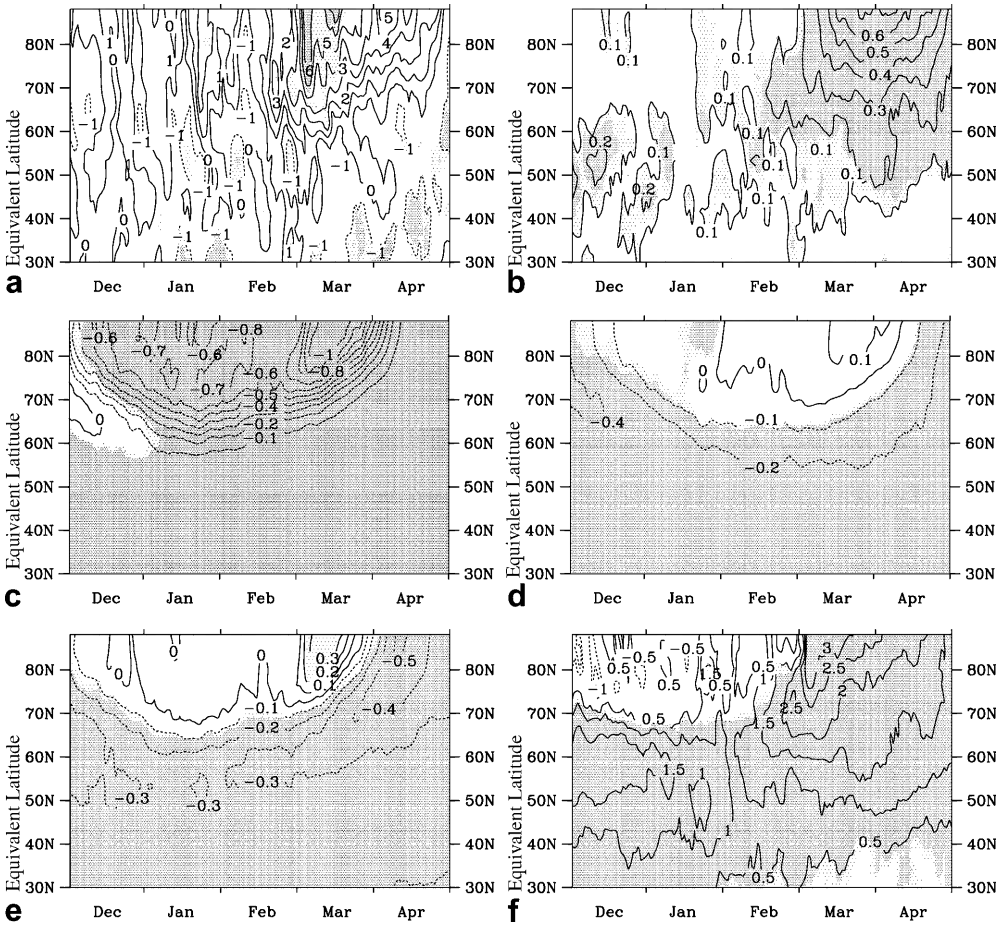

Fig. 11a–f Same as Fig. 10, but in the Northern Hemisphere from December to April

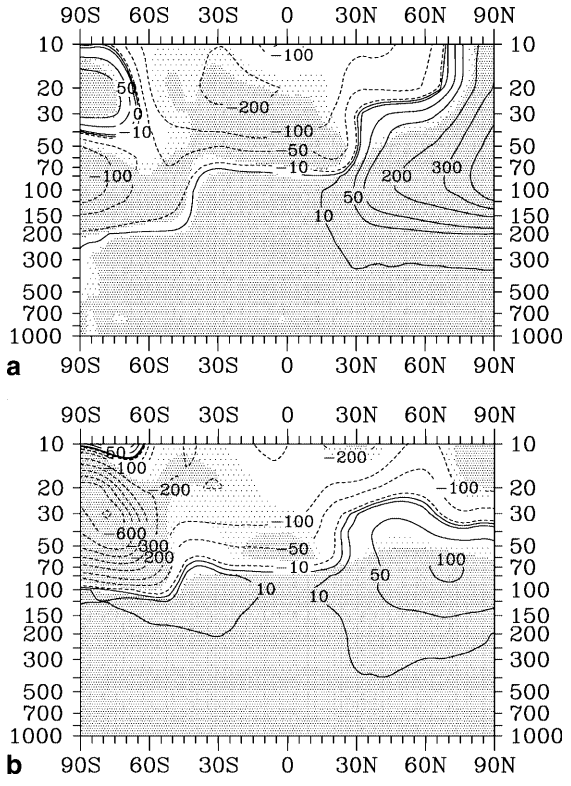

Fig. 12a,b Changes of the climatological zonal mean ozone mixing ratios (in ppbv) for the "2015" and the "1990" simulation depending on altitude and latitude for **a** March and **b** October. *Negative (positive) values* indicate higher (lower) values in "1990" ("2015"). *Heavy (light) shaded areas* indicate the 99% (95%) significance level (*t*-test)

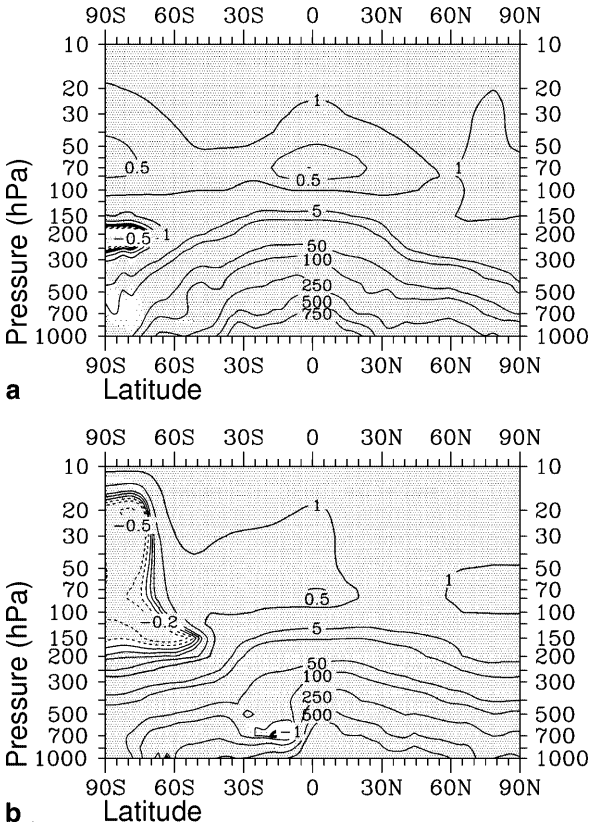

Fig. 13a,b Changes of the climatological mean water vapor mixing ratios (in ppmv) between "2015" and "1990" for **a** DJF and **b** JJA (see Fig. 6). *Positive values* indicate an increase of mixing ratios from "1990" to "2015"

dynamic processes, which quantify the causes and effects involved in the net development of the ozone layer.

4.1 Stratospheric temperature adjustment

To analyze the origin of the warming of the polar lower stratosphere in Northern Hemisphere late winter (Fig. 8a), it is quite helpful to contemplate the stratosphere adjusted temperature during that season (Fig. 14). The stratospheric adjustment is merely a by-product of the adjusted radiative forcing calculation (see earlier), but it provides a good first-order estimation of the stratospheric net temperature response (e.g. Rosier and Shine 2000). It reflects the purely radiative impact of all trace gas changes (including ozone) to the stratospheric temperature. This effect is evidently a cooling one and extends over the whole stratosphere including the northern polar latitudes. Though the stratospheric ozone increase in the Northern Hemisphere makes a warming contribution (not shown), this is reversed by the negative contributions from CO_2 and stratospheric water vapor increase. Hence it is indicated that the net warming to be noticed in Fig. 8a can only be caused by dynamic feedbacks within the fully interactive system, and not by the primary radiative effect of the trace gas changes. A general discussion of the competing radiative effects of the various trace gas changes is beyond our scope and will be presented elsewhere (Ponater et al., in preparation) in sufficient detail.

Table 2 Stratosphere adjusted radiative forcing of the simulated stratospheric ozone and water vapor changes and of all radiatively active tracer changes considered (also including those of CO_2, N_2O, CH_4, and CFCs)

	1990	2015
Stratospheric ozone	–0.02	+0.02
Stratospheric water vapor	+0.04	+0.24
All gases	+0.37	+1.69

4.2 Analysis of meridional eddy heat flux and streamfunction

To explain the different temperature response in both hemispheres for the "2015" scenario, the impact of the dynamic processes must be equal or larger than the radiative effect in the Northern Hemisphere polar winter and spring.

The dynamic forcing of the stratosphere is strongly influenced by large-scale planetary waves generated by

topography and land-sea temperature differences. Fundamental differences in the surface topography lead to a more pronounced wave activity in the Northern than in the Southern Hemisphere. Land-sea temperature gradients are different in our three model simulations, which then could cause a different forcing of planetary waves in each model run. The variability of the winter polar vortices and their breakdown (final warming) is clearly associated with planetary wave forcing, particularly with stationary waves. The strength of wave forcing can be determined in various ways. One possibility to estimate the wave flux from the troposphere into the stratosphere is to calculate the meridional eddy heat flux, which is proportional to the vertical component of the Eliassen Palm (EP) flux (Andrews et al. 1987).

Figure 15 shows the calculated meridional heat flux by stationary eddies for the "1990" reference simulation (Fig. 15a), and the differences with respect to the "1980" (Fig. 15b) and the "2015" model experiment (Fig. 15c) for Northern Hemisphere winter conditions (DJF). Positive values in the winter hemisphere indicate a northward heat flux (Fig. 15a) that gradually intensifies from "1980" to "1990" (Fig. 15b) and "2015" (Fig. 15c), respectively. The modification of the meridional heat flux from "1980" to "1990" is insignificant both in the stationary and in the transient component (not shown). The stationary wave activity is enhanced in "2015", most pronounced around 60°N in the lower stratosphere. No significant changes of the transient component of the poleward heat flux are evident (not shown). The strengthening of the heat flux in "2015" with respect to "1990" should lead to enhanced wave breaking in the lower stratosphere and enhanced mixing across the edge of the polar vortex (e.g. Coy et al. 1997). As indicated in Fig. 8a, the Northern Hemisphere winter is more disturbed, and the polar vortex in "2015" decays earlier than in "1990", which is in consistent with the explanations just mentioned. As a consequence, temperatures increase after mid February through dynamic processes (see Sect. 4.1). Comparing the number of Northern Hemisphere stratospheric warming events (minor, major, major final) between the "1990" and the "2015" simulations (see also H2001) the number of warmings are increased by approximately 40% in the "2015" simulation (not shown). Therefore, the intensified variability of the vortex can be mainly attributed to a stronger wave activity in the winter season. In Southern Hemisphere winter no significant changes of wave activity occur (not shown), either between the "1980" and "1990" experiments, or between the "1990" and "2015" simulations. Hence, there is no process to prevent the development of an extended and more persistent vortex in spring, which is caused by greenhouse gas increase and the enlarged ozone hole.

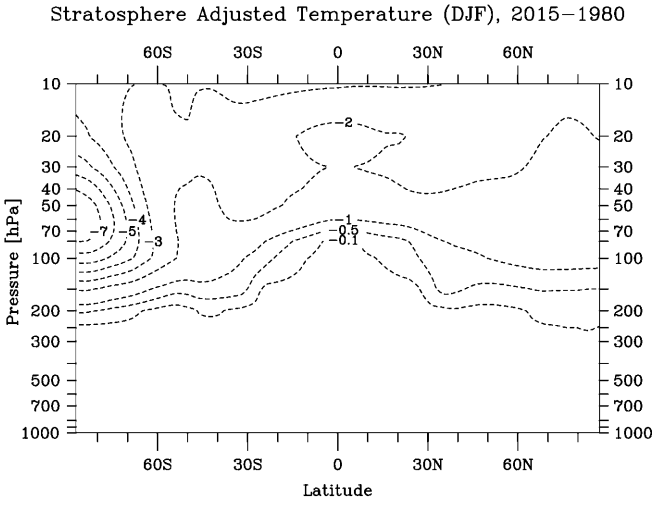

Fig. 14 Changes of the adjusted temperature of the lower stratosphere between "2015" and "1980" in Northern Hemisphere winter time (DJF). *Negative values* indicate a cooling from "1980" to "2015" (see text)

To complete the analysis of dynamic changes in the different model experiments, the residual meridional circulation streamfunction is investigated for Northern Hemisphere winter conditions, based on climatological mean values of the "1990" reference simulation and the respective differences to "1980" and "2015" (Fig. 16). The result for the reference simulation (Fig. 16a) is in qualitative agreement with published work (e.g. Rosenlof 1995; Manzini and McFarlane 1998). Obviously, the winter hemisphere cell is stronger than the cell in the summer hemisphere. Air masses ascend in the tropics into the lower stratosphere and descend at middle and high latitudes. The model produces the strongest subsidence inside the vortex, which is in agreement with analyses (e.g. Schoeberl et al. 1992; Manney et al. 1994b). When contemplating the mean vertical wind velocity in the E39/C reference simulation (not shown), weaker descent is found inside the polar vortex near the model top compared with deeper model layers: at 20 hPa, the mean downward motion varies between –0.05 (vortex core) and –0.07 cm/s (inner edge of the vortex), whereas at 50 hPa it is between –0.08 and –0.1 cm/s. The values at 50 hPa are in agreement with estimates using observations of passive tracers (H2001). This model result indicates an inconsistency with the observations, which show a general decrease of downward velocities with increasing density. This could have an impact on the results. On the other hand, even though the vertical velocities near the model top are too small, they are not totally unrealistic, i.e. not showing an upward movement of mass, as episodically found in earlier model versions (e.g. Steil et al. 1998). The agreement between modelled vertical velocities and respective analyses at 50 hPa indicates that the wintertime lower stratospheric dynamics at middle and high latitudes of the Northern Hemisphere are not exclusively dominated from above (downward control principle). The results rather suggest that planetary wave forcing could play an essential role in determining the dynamic structure of the lower stratosphere during the winter season. Considering the differences of the residual circulation streamfunction between the reference run and the "1980" and the

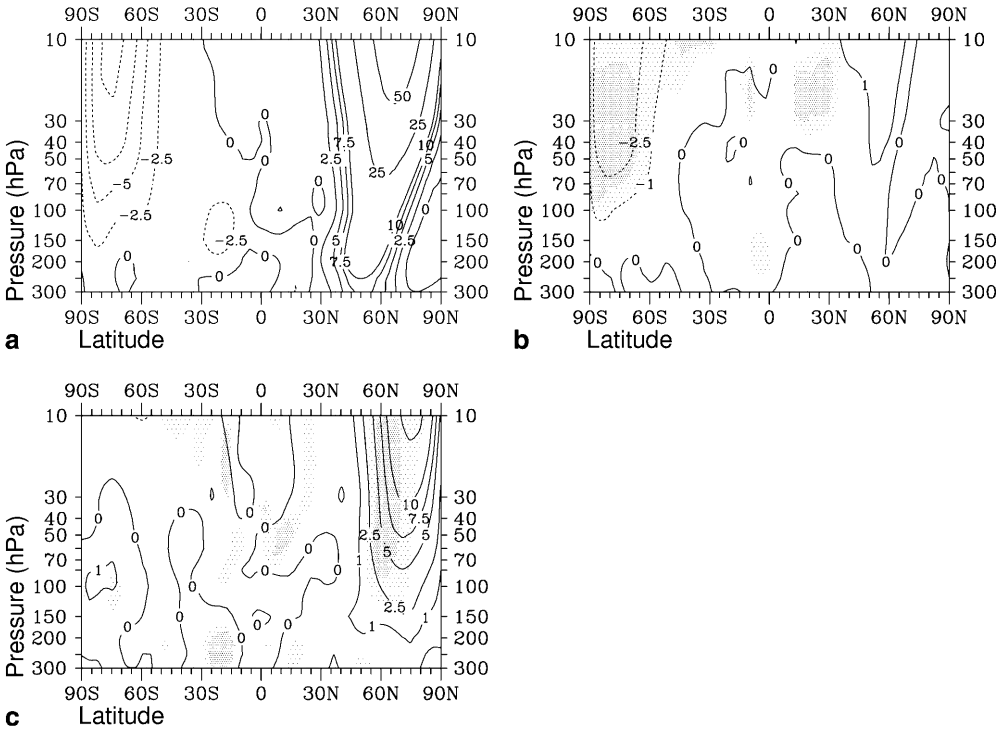

Fig. 15 **a** Zonal mean values of the meridional heat flux by stationary eddies in northern winter (DJF) for the "1990" reference simulation, depending on altitude and latitude (in K m/s). *Positive (negative) values* in the Northern (Southern) Hemisphere indicate a poleward transport of heat. **b** Differences between "1990" and "1980" and **c** between "2015" and "1990"; positive values in the Northern Hemisphere indicate an intensified poleward transport in "1990" and in "2015", respectively. *Heavy (light) shaded areas* indicate the 99% (95%) significance level (*t*-test)

"2015" simulations, respectively, E39/C calculates an enhancing residual circulation in middle latitudes of the lower winter stratosphere in response to increasing greenhouse gases (statistically significant only in Fig. 16c, displaying the change between "1990" and "2015"), which causes a stronger mass transport to high latitudes. The model results concerning the residual circulation streamfunction and its temporal change indicate a consistent behavior with middle atmosphere GCMs (WMO 1999, see page 12–26). For example, employing the GISS GCM, Rind et al. (1998) carried out a doubled CO_2 experiment, in which a warming of the extra-tropical winter stratosphere was produced, associated with an increased residual circulation.

5 Conclusions

New results of the global chemistry-climate model E39/C have been presented, which incorporate the interaction of radiative, chemical, and dynamic processes. Model data have been compared with observations, and differences in the diverse simulations have been analyzed.

Inspections of observations have indicated that particularly the polar lower stratosphere has significantly cooled during the first half of the 1990s resulting in a strengthened persistence of the polar vortices, not only in the Southern, but also in the Northern Hemisphere (e.g. Randel and Wu 1999, Zhou et al. 2000). The model reproduces this behavior in the Southern Hemisphere where the dynamic variability caused by planetary wave activity plays only a minor role. This supports the hypothesis that the increased persistence of the polar vortex is mainly due to the strong ozone depletion in the Antarctic lower stratosphere observed in the recent two decades. The "2015" sensitivity simulation shows that this behavior could continue over the coming years.

In the Northern Hemisphere, a slightly enhanced persistence of the vortex in "1990" is also simulated with respect to "1980", again caused by radiative cooling due to reduced stratospheric ozone and enhanced greenhouse gas concentrations. A different picture evolves for the situation in "2015": in winter, planetary wave activity is enhanced leading to a more disturbed vortex. The dynamical heating compensates the radiative cooling due to enhanced greenhouse gas concentrations. Hence, the net temperature changes simulated in the polar region are not statistically significant. Reduced Cl_y loading then leads to less chlorine activation and, thus, significantly less ozone depletion is found in spring. Enhanced planetary wave activity and higher ozone mixing ratios together yield a strong temperature increase in March, resulting in an earlier final warming.

It should be emphasized that the "2015" simulation must been seen as a sensitivity experiment of our model system and not as a reliable prognosis for the future development of atmospheric composition and climate. The simulations neglect important natural processes, which could have an impact on the behavior of the atmosphere, i.e. eruptions of volcanoes, the 11-year solar activity cycle, or the QBO. We have demonstrated that the model results regarding the past time qualitatively agree with observations, putting the "2015" results on a consolidated basis. Nevertheless, how the atmosphere will develop in future is still an open question. One key parameter is stratospheric temperature. Climate models generally predict a cooling of the Southern Hemisphere stratosphere, which may delay the recovery of the ozone

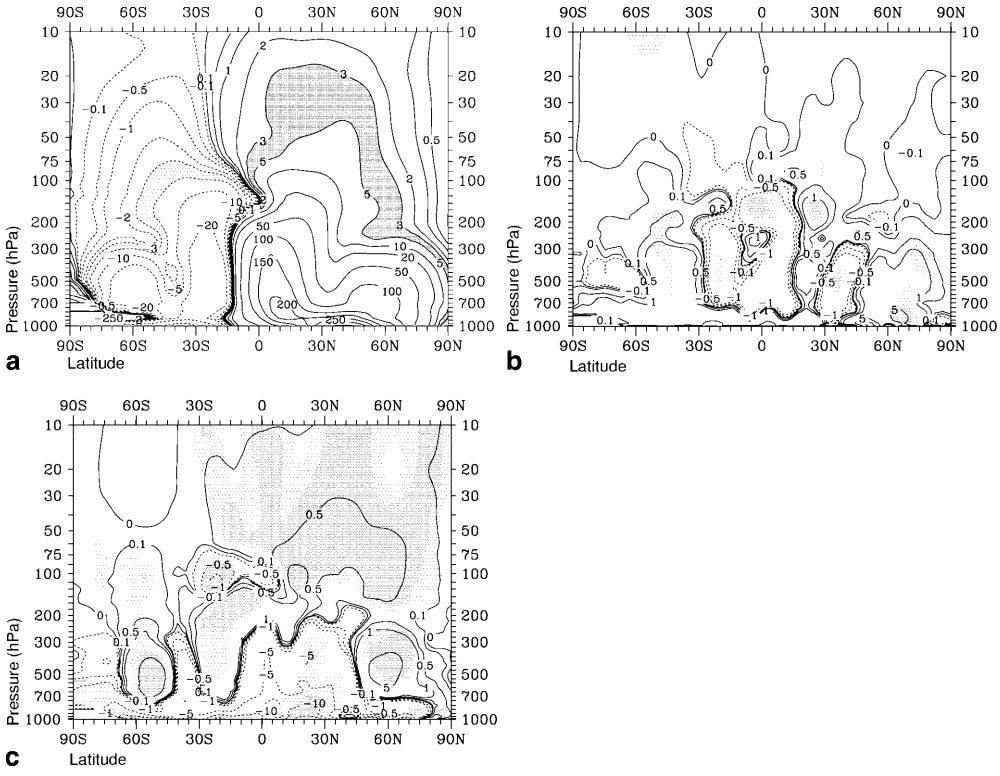

Fig. 16 **a** Contours of the climatological residual circulation streamfunction in northern winter (DJF) for the "1990" simulation, depending on altitude and latitude (in 10^9 kg/s). *Positive (negative) values* in the Northern (Southern) Hemisphere indicate a clockwise (counterclockwise) circulation. **b** Differences between "1990" and "1980" and **c** between "2015" and "1990"; positive values in the Northern Hemisphere indicate a greater clockwise circulation. *Heavy (light) shaded areas* indicate the 99%-(95%-) significance level (*t*-test)

layer (Shindell et al. 1998; Austin et al. 2000). However, a temperature prognosis for the Northern Hemisphere is much more complicated than for the Southern Hemisphere since dynamics play such an important role. This is indicated by various climate studies, in which contrasting stratospheric temperature developments are simulated (cooling: Austin and Butchart 1994; Shindell et al. 1998, warming: Mahfouf et al. 1994; Rind et al. 1998). Another limitation of the current study with respect to future estimates is the fact that at present CHEM does not include bromine chemistry. This could have an influence on calculated ozone depletion rates, particularly in future, although bromine compounds are considered in international ozone layer protecting agreements.

A more detailed analysis of the dynamic-chemical feedback mechanisms is required to answer the remaining questions, particularly with respect to the possible change of planetary wave activity and corresponding temperature development in the lower stratosphere. The future application of coupled chemistry-climate models will help to get a better understanding of the mutual effects, which can support the analysis of observations and which can be used for more reliable estimates of the possible future development of the atmosphere. As shown by H2001 and the results presented here, chemistry-climate models with a model top centred at 10 hPa and an adequate spatial resolution, particularly in the vertical, can also provide fundamental contributions regarding the dynamics and chemistry of the troposphere and the lower stratosphere. Of course, it cannot be guaranteed that a model which reproduces observations fairly well produces reliable estimates for the future development of atmospheric conditions. However, the model results presented give some interesting indications, which must be critically discussed and compared with similar assessments of other model approaches.

Acknowledgement This study was supported by the Bundesministerium für Bildung und Forschung (07DLR02). We thank the staff of T-Systems debis Systemhaus SfR, Oberpfaffenhofen, Germany, for support in using computer facilities. E. Roeckner and M. Esch are kindly acknowledged for providing sea surface temperature data from their coupled ocean-atmosphere model. We also thank the HALOE science team for providing their observational data.

References

Andrews DG, Holton JR, Leovy CB (1987) Middle atmosphere dynamics. Academic, Orlando, 489 pp

Austin J, Butchart N, Shine K (1992) Possibility of an Arctic ozone hole in a doubled CO_2 climate. Nature 360: 221–225

Austin J, Butchart N (1994) The influence of climate change and the timing of stratospheric warmings on Arctic ozone depletion. J Geophys Res 99: 1127–1145

Austin J, Butchart N, Swinbank RS (1997) Sensitivity of ozone and temperature to vertical resolution in a GCM with coupled stratospheric chemistry. Q J R Meteorol Soc 123: 1405–1431

Austin J, Knight J, Butchart N (2000) Three-dimensional chemical model simulations of the ozone layer: 1979–2015. Q J R Meteorol Soc 126: 1533–1556

Bengtsson L, Roeckner E, Stendel M (1999) Why is the global warming proceeding much slower than expected?. J Geophys Res 104: 3865–3876

Benkovitz CM, Scholtz MT, Pacyna J, Tarrason L, Dignon J, Voldner EC, Spiro PA, Logan JA, Graedel TE (1996) Global gridded inventories of anthropogenic emissions of sulfur and nitrogen. J Geophys Res 101: 29239–29253

Boughner RE (1978) The effect of increased carbon dioxide concentrations on stratospheric ozone. J Geophys Res 83: 1326–1332
Brühl C, Crutzen PJ (1993) MPIC two-dimensional model. NASA Ref Publ 1292: 103–104
Butchart N, Remsberg EE (1986) The area of the stratospheric polar vortex as a diagnostic for tracer transport on an isentropic surface. J Atmos Sci 43: 1319–1339
Cariolle D, Lasserre-Bigorry A, Royer J-F, Geleyn J-F (1990) A GCM simulation of the springtime Antarctic ozone decrease and its impact on mid-latitudes. J Geophys Res 95: 1883–1898
Chipperfield MP, Pyle JA (1998) Model sensitivity studies of arctic ozone depletion. J Geophys Res 103: 28389–28403
Coy L, Nash ER, Newman PA (1997) Meteorology of the polar vortex: spring 1997. Geophys Res Lett 24: 2693–2696
Dameris M, Berger U, Günther G, Ebel A (1991) The ozone hole: dynamical consequences as simulated with a three-dimensional model of the middle atmosphere. Ann Geophys 9: 661–668
Dameris M, Grewe V, Hein R, Schnadt C, Brühl C, Steil B (1998) Assessment of the future development of the ozone layer. Geophys Res Lett 25: 3579–3582
Danilin MY, Sze N-D, Ko MKW, Rodriguez JM, Tabazadeh A (1998) Stratospheric cooling and Arctic ozone recovery. Geophys Res Lett 25: 2141–2144
Douglass AR, Schoeberl MR, Stolarski RS, Waters JW, Russell III JM, Roche AE, Massie ST (1995) Inter-hemispheric differences in springtime production of HCl and $ClONO_2$ in the polar vortices. J Geophys Res 100: 13967–13978
Fels SB, Mahlmann JD, Schwarzkopf MD, Sinclair RW (1980) Stratospheric sensitivity to perturbations in ozone and carbon dioxide: radiative and dynamical response. J Atmos Sci 37: 2265–2297
Forster PM de F (1999) Radiative forcing due to stratospheric ozone changes 1979–1997, using updated trend estimates. J Geophys Res 104: 24 395–24399
Gates WL (1992) AMIP: the atmosphere model inter-comparison project. Bull Am Meteorol Soc 73: 1962–1970
Graf H-F, Kirchner I, Perlwitz J (1998) Changing lower stratospheric circulation: the role of ozone and greenhouse gases. J Geophys Res 103: 11251–11261
Grewe V, Dameris M, Sausen R, Steil B (1998) Impact of stratospheric dynamics and chemistry on northern hemisphere midlatitude ozone loss. J Geophys Res 103: 25417–25433
Grewe V, Dameris M, Hein R, Sausen R, Steil B (2001) Future changes of the atmospheric composition and the impact of climate change. Tellus 53B: 103–121
Groves KS, Mattingly SR, Tuck AF (1978) Increased atmospheric carbon dioxide and stratospheric ozone. Nature 273: 711–715
Hartmann DL, Wallace JM, Limpasuvan V, Thomson DWJ, Holton JR (2000) Can ozone depletion and global warming interact to produce rapid climate change? PNAS 97: 1412–1417
Hein R, Dameris M, Schnadt C, Land C, Grewe V, Köhler I, Ponater M, Sausen R, Steil B, Landgraf J, Brühl C (2001) Results of an interactively coupled chemistry-general circulation model: comparison with observations. Ann Geophys 19: 435–457
Huntrieser H, Schlager H, Feigl C, Höller H (1998) The transport and production of NO_x in electrified thunderstorms: survey of previous studies and new observations at mid-latitudes. J Geophys Res 103: 28247–28264
IPCC (1990) (Intergovernmental Panel on Climate Change) Climate change, The IPCC Scientific Assessment. Houghton JT et al. (eds) Cambridge University Press, Cambridge
IPCC (1995) (Intergovernmental Panel on Climate Change) Climate change 1994, Radiative forcing of climate change. Houghton JT et al. (eds) Cambridge University Press, Cambridge
IPCC (1996) (Intergovernmental Panel on Climate Change) Climate change 1995, The science of climate change. Houghton JT et al. (eds) Cambridge University Press, Cambridge
IPCC (1999) (Intergovernmental Panel on Climate Change) Aviation and the global atmosphere. Penner JE, Lister DH, Griggs DJ, Dokken DJ, McFarland M (eds) Cambridge University Press, Cambridge
Kivi R, Kyrö E, Turunen T, Ulich T, Turunen E (1999) Atmospheric trends above Finland: II. Troposphere and stratosphere. Geophysica 35: 71–85
Labitzke K, van Loon H (1994) Trends of temperature and geopotential height between 100 and 10 hPa in the northern hemisphere. J Meteorol Soc Japan 72: 643–652
Labitzke K, van Loon H (1995) A note on the distribution of trends below 10 hPa: the extra-tropical northern hemisphere. J Meteorol Soc Jpn 73: 883–889
Land C, Ponater M, Sausen R, Roeckner E (1999) The ECHAM4.L39(DLR) atmosphere GCM – Technical description and model climatology. DLR-Oberpfaffenhofen, Rep 1991–31, Wessling, Germany, ISSN 1434–8454
Langematz U (2000) An estimate of the impact of observed ozone losses on stratospheric temperature. Geophys Res Lett 27: 2077–2080
Mahfouf JF, Cariolle D, Royer J-F, Geleyn J-F, Timbal B (1994) Response of the meteo-France climate model to changes in CO_2 and the sea surface temperature. Clim Dyn 9: 345–362
Manney GL, Zurek RW, Gelman ME, Miller AJ, Nagatani R (1994a) The anomalous Arctic lower stratospheric polar vortex. Geophys Res Lett 21: 2405–2408
Manney GL, Zurek RW, O'Neill A, Swinbank R (1994b) On the motion of air through the stratospheric polar vortex. J Atmos Sci 51: 2973–2994
Manzini E, McFarlane NA (1998) The effect of varying the source spectrum of a gravity wave parameterization in a middle atmosphere general circulation model. J Geophys Res 103: 31523–31539
McPeters RD, Hollandsworth SM, Flynn LE, Herman JR, Seftor CJ (1996) Long-term ozone trends derived from the 16-year combined Nimbus 7/Meteor 3 TOMS version 7 record. Geophys Res Lett 23: 3699–3702
Montzka SA, Butler JH, Myers RC, Thompson TM, Swanson TH, Clarke AD, Lock LT, Elkins JW (1996) Decline in the tropospheric abundance of halogen from halocarbons: implications for stratospheric ozone depletion. Science 272: 1318–1322
Montzka SA, Butler JH, Elkins JW, Thompson TM, Clarke AD, Lock LT (1999) Present and future trends in the atmospheric burden of ozone-depleting halogens. Nature 398: 690–694
Oltmans SJ, Hofmann DJ (1995) Increase in lower stratospheric water vapor at mid-latitude northern hemisphere site from 1981 to 1994. Nature 374: 146–149
Pawson S, Labitzke K, Leder S (1998) Stepwise changes in stratospheric temperatures. Geophys Res Lett 25: 2157–2160
Pawson S et al. (2000) The GCM-reality inter-comparison project of SPARC (GRIPS): scientific issues and initial results. Bull Am Meteorol Soc 81: 781–796
Perlwitz J, Graf H-F (1995) The statistical connection between tropospheric and stratospheric circulation of the northern hemisphere in winter. J Clim 8: 2281–2295
Perlwitz J, Graf H-F, Voss R (2000) The leading mode of the coupled troposphere-stratosphere winter circulation in different climate regimes. J Geophys Res 105: 6915–6926
Pitari G, Palermi S, Visconti G (1992) Ozone response to a CO_2 doubling: results from a stratospheric circulation model with heterogeneous chemistry. J Geophys Res 97: 5953–5962
Price C, Rind D (1992) A simple lightning parameterization for calculating global lightning distributions. J Geophys Res 97: 9919–9933
Price C, Rind D (1994) Modeling global lightning distributions in a general circulation model. Mon Weather Rev 122: 1930–1937
Ramanathan V, Callis LB, Boughner RE (1976) Sensitivity of surface temperature and atmospheric temperature to perturbations in the stratospheric concentration of ozone and nitrogen dioxide. J Atmos Sci 33: 1092–1112
Randel WJ, Wu F (1999) Cooling of the Arctic and Antarctic polar stratosphere due to ozone depletion. J Clim 12: 1467–1479

Rind D, Suozzo R, Balachandran NK, Prather MJ (1990) Climate change and the middle atmosphere. Part I: the doubled CO_2 climate. J Atmos Sci 47: 475–494

Rind D, Shindell D, Lonergan P, Balachandran NK (1998) Climate change and the middle atmosphere: Part III, The doubled CO_2 climate revisited. J Clim 11: 876–894

Roeckner E, Bengtsson L, Feichter J, Leliefeld J, Rodhe H (1999) Transient climate change simulations with a coupled atmosphere-ocean GCM including the tropospheric sulfur cycle. J Clim 12: 3003–3032

Rosenlof KH (1995) Seasonal cycle of the residual mean meridional circulation in the stratosphere. J Geophys Res 100: 5173–5191

Rosier SM, KP Shine (2000) The effect of two decades of ozone changes on stratospheric temperature as indicated by a general circulation model. Geophys Res Lett 27: 2617–2620

Santee ML, Manney GL, Froidevaux L, Read WG, Waters JW (1999) Six years of UARS Microwave Limb Sounder HNO_3 observations: seasonal, inter-hemispheric, and inter-annual variations in the lower stratosphere. J Geophys Res 104: 8225–8246

Santer BD, Hnilo JJ, Wigley TML, Boyle JS, Doutriaux C, Fiorino M, Parker DE, Taylor KE (1999) Uncertainties in observationally based estimates of temperature changes in the free atmosphere. J Geophys Res 104: 6305–6333

Schmitt A, Brunner B (1997) Emissions from aviation and their development over time. In: Schumann U. et al. (ed) Pollutants from air traffic – results from atmospheric research 1992–1997, DLR-Mitteilungen, 97–04, DLR-Köln, Germany, pp 37–52

Schoeberl MR, Lait LR, Newman PA, Rosenfield JE (1992) The structure of the polar vortex. J Geophys Res 97: 7859–7882

Shindell DT, Rind D, Lonergan P (1998) Increased polar stratospheric ozone losses and delayed eventual recovery owing to increasing greenhouse-gas concentrations. Nature 392: 589–592

Shine KP (1986) On the modelled thermal response of the Antarctic stratosphere to a depletion of ozone. Geophys Res Lett 13: 1331–1334

Shine KP (1989) Sources and sinks of zonal momentum in the middle atmosphere using the diabatic circulation. Q J R Meteorol Soc 115: 265–292

Steil B, Dameris M, Brühl C, Crutzen PJ, Grewe V, Ponater M, Sausen R (1998) Development of a chemistry module for GCMs: first results of a multi-annual integration. Ann Geophys 16: 205–228

Steinbrecht W, Claude H, Köhler U, Hoinka KP (1998) Correlations between tropopause height and total ozone: implications for long-term changes. J Geophys Res 103: 19183–19192

Stuber N, Sausen R, Ponater M (2001) Stratosphere adjusted radiative forcing calculations in a comprehensive climate model. Theor Appl Climatol 68: 125–135

Timmreck C, Graf H-F, Feichter J (1999) Simulation of Mt. Pinatubo volcanic aerosol with the Hamburg climate model ECHAM4. Theor Appl Climatol 62: 85–108

Toon GC, Farmer CB, Lowes LL, Schaper PW, Blavier J-F, Norton RH (1989) Infrared aircraft measurements of stratospheric composition over Antarctica during September 1987. J Geophys Res 94: 16571–16596

WMO (1998) (World Meteorological Organisation) Assessment of trends in the vertical distribution of ozone. SPARC Report 1, Ozone Research and Monitoring Project, Report 43

WMO (1999) (World Meteorological Organisation) Scientific assessment of ozone depletion: 1998. Global Ozone Research and Monitoring Project, Report 44

Zhou S, Gelman ME, Miller AJ, McCormack JP (2000) An interhemispheric comparison of the persistent stratospheric polar vortex. Geophys Res Lett 27: 1123–1126